TOXICOLOGICAL SCIENCES **100(1)**, 203–214 (2007)
doi:10.1093/toxsci/kfm196
Advance Access publication July 28, 2007

Pulmonary and Systemic Immune Response to Inhaled Multiwalled Carbon Nanotubes

Leah A. Mitchell,*,† Jun Gao,* Randy Vander Wal,‡ Andrew Gigliotti,† Scott W. Burchiel,* and Jacob D. McDonald†,[1]

*College of Pharmacy, University of New Mexico, Albuquerque, New Mexico 87131–0001; †Lovelace Respiratory Research Institute, Albuquerque, New Mexico 87108; and ‡The National Center for Microgravity Research, c/o The NASA-Glenn Research Center, Cleveland, Ohio 44135

Received May 27, 2007; accepted July 18, 2007

Inhalation of multiwalled carbon nanotubes (MWCNTs) at particle concentrations ranging from 0.3 to 5 mg/m^3 did not result in significant lung inflammation or tissue damage, but caused systemic immune function alterations. C57BL/6 adult (10- to 12-week) male mice were exposed by whole-body inhalation to control air or 0.3, 1, or 5 mg/m^3 respirable aggregates of MWCNTs for 7 or 14 days (6 h/day). Histopathology of lungs from exposed animals showed alveolar macrophages containing black particles; however, there was no inflammation or tissue damage observed. Bronchial alveolar lavage fluid also demonstrated particle-laden macrophages; however, white blood cell counts were not increased compared to controls. MWCNT exposures to 0.3 mg/m^3 and higher particle concentrations caused nonmonotonic systemic immunosuppression after 14 days but not after 7 days. Immunosuppression was characterized by reduced T-cell–dependent antibody response to sheep erythrocytes as well as T-cell proliferative ability in presence of mitogen, Concanavalin A. Assessment of nonspecific natural killer (NK) cell activity showed that animals exposed to 1 mg/m^3 had decreased NK cell function. Gene expression analysis of selected cytokines and an indicator of oxidative stress were assessed in lung tissue and spleen. No changes in gene expression were observed in lung; however, interleukin-10 (IL-10) and NAD(P)H oxidoreductase 1 mRNA levels were increased in spleen.

Key Words: **carbon nanotubes; inhalation; pulmonary pathology; immunosuppression.**

Carbon nanotubes (CNTs) are among the most promising and unique engineered nanomaterials. The global production of CNTs has already reached hundreds of metric tons per year and is expanding rapidly as new applications and manufacturers develop (Harper and Vas, 2005). No other material has been developed that possesses the size (1–20 nm in width, and many microns in length), strength, and surface chemistry properties of CNTs. Many of the properties that make CNTs remarkable for engineering applications have also caused concern for their biocompatibility, especially in the lung. Their length/width (aspect) ratios of > 1000, reactive surface chemistry, and poor solubility raise concerns linked to past experience with hazardous fibers (e.g., asbestos). Persistent reactive fibers lead to oxidative reactions that result in lung injury (McClellan, 1994). The relevance of findings from fiber toxicity studies to the biocompatibility of CNTs has been suggested (Huczko *et al.*, 2001; Magrez *et al.*, 2006) but is not well established.

Early studies demonstrated that CNTs induced pulmonary injury, including fibrosis, when instilled into rodent lungs. In 2006, Lam *et al.* published a comprehensive review on the sources, characteristics, and toxicology of CNTs. Of particular note is that CNTs exist in many forms, including single-walled carbon nanotubes (SWCNTs), double-walled CNTs, and multiwalled carbon nanotubes (MWCNTs). In addition to the potential for occupational exposure, environmental exposures to low concentrations of MWCNTs, but not SWCNTs, have been reported (Murr *et al.*, 2005). The presence of MWCNTs in the environment was reported to be due to combustion emissions, as they have been found in the effluent from natural gas combustion.

Biological and toxicological responses to CNTs may vary by dose, route of dosing, and type of CNTs. Reported research on the pulmonary *in vivo* toxicity of CNTs to date has been conducted by either instillation into the trachea (Lam *et al.*, 2004; Muller *et al.*, 2005; Warheit *et al.*, 2004) or pharyngeal aspiration (Shvedova *et al.*, 2005). Each of these publications reported significant pulmonary effects, including inflammation, evidence of oxidative stress, fibrosis (Shvedova *et al.*, 2005), and granuloma formation (Lam *et al.*, 2004; Muller *et al.*, 2005; Shvedova *et al.*, 2005; Warheit *et al.*, 2004). Warheit *et al.* (2004) reported multifocal granulomas in the absence of a linear dose-response changes in lavage parameters and uniformity of lesions. These transient, nonmonotonic responses were potentially attributed to the artificial route of dosing bolus material to the lung by instillation. Shvedova *et al.* (2005) reported improved linearity in dose-response relationships and the additional observation of fibrotic injury that was attributed to an improved lung delivery by pharyngeal aspiration.

CNT biocompatibility studies conducted to date form an initial basis for evaluating the hazard of CNTs. However, the

[1] To whom correspondence should be addressed at Lovelace Respiratory Research Institute, 2425 Ridgecrest Drive SE, Albuquerque, NM 87108. Fax: (505) 348-4980. E-mail: jmcdonal@lrri.org.

need to conduct inhalation exposures (as opposed to instillation or aspiration) to CNTs to place these prior results in context has been stated by several investigators (Kipen and Laskin, 2005; Lam *et al*., 2006; Warheit *et al*., 2004). To this end, we have developed an inhalation exposure system for the conduct of whole-body inhalation exposure of rodents to CNTs. The exposure system was developed to produce CNT aerosols that simulate resuspended CNT powders that may exist in the workplace. While only limited data exist on the potential for pulmonary exposure in the workplace, Maynard *et al*. (2004) showed the feasibility and characteristics of aerosolized CNTs produced from mechanical agitation. In that study, approximately 50 $\mu g/m^3$ of CNTs was produced, and the particle size changed with the degree of agitation. In general, a bimodal particle size distribution was observed with some particles < 100 nm and the majority at approximately 300–600 nm. For the present study, we attempted to approximate the size distribution observed by Maynard *et al*. (2004). Although that study used SWCNTs, the current study used MWCNTs because they are produced in higher production volumes and we could obtain large quantities of commercial grade, high-quality MWCNTs.

This study was conducted to assess short-term pulmonary and systemic immune response to inhaled MWCNTs as a function of dose and time. Pulmonary toxicity evaluations were conducted in view of previous reports of significant inflammation and tissue injury observed in short time periods after dosing. Standard measurements of pulmonary injury, including histopathology, white blood cell count in bronchial alveolar lavage fluid (BALF), and some measurements of oxidative stress and cytokine induction were used. In addition to the pulmonary response to MWCNTs, we explored the ability of MWCNTs to cause systemic immune suppression, a response we have previously reported from inhalation of environmental pollutants at low concentrations (Burchiel *et al*., 2004, 2005). Moreover, immune suppression has also been reported following asbestos inhalation (Magrez *et al*., 2006; Rosenthal *et al*., 1998). The overall goal of this study was to develop a suitable aerosol delivery and inhalation system, and apply that system to characterize the pulmonary and systemic immune response after short-term (up to 14 days) inhalation exposures of mice.

MATERIALS AND METHODS

Study design. The study design and a summary of the measurements are provided in Figure 1. Mice were housed and exposed in whole-body inhalation exposure chambers for 7 or 14 consecutive days. During exposure, aerosolized MWCNTs were sampled from within each chamber for characterization. MWCNT material was imaged by scanning and transmission electron microscopy (SEM and TEM, respectively). Impurities, functional groups, and metals were measured by x-ray photoemission and energy-dispersive spectroscopy. The aerosol particle size distribution was also analyzed. After exposure, animals were removed from the chamber and sacrificed the following morning. All pulmonary and systemic end points listed in Figure 1 were carried out in 7- and 14-day–exposed animals. Lung end points included BALF cellularity, histopathology, and gene expression analysis. Spleen, a representative organ for analysis of systemic immunity, was analyzed for T-cell–dependent antibody response, T- and B-cell proliferative ability, a marker of innate immune function, and gene expression. Splenic interleukin (IL-10) gene expression was further validated by IL-10 protein analysis, only 14-day data are shown. Details on the methodology are described below.

Source and characteristics of MWCNTs. Dispersible MWCNTs were purchased from Shenzhen Nanotech Port Co. (Shenzhen, China). These MWCNTs were engineered in high yield from a proprietary chemical vapor

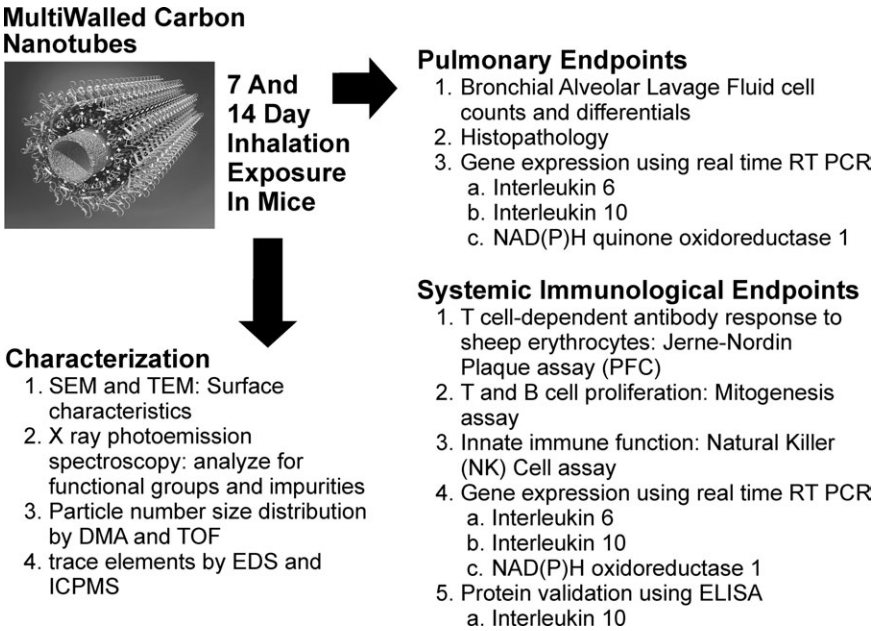

FIG. 1. Study design.

TABLE 1
MWCNT Characterization

Characteristics	Manufacturer's specifications	Measured characteristics
Purity	> 95%	
Diameter	10–20 nm	10–20 nm
Length	5–15 μm	
Amorphous carbon	< 3%	
Ash (catalyst residue)	< 0.2%	
Surface area	40–300 m^2/g	100 m^2/g
Thermal conductivity	~2000 W/m·k	
Carbon		97.90%
Oxidized carbon		2.10%
Metal impurities		
Nickel		0.50%
Iron		0.50%

deposition (CVD) process. Additional characterization of the bulk MWCNTs was conducted, including determination of chemical composition of ash impurities, residual catalyst, and oxygen functional groups. Functional group impurities were assessed by x-ray photoemission spectroscopy (XPS). A PHI 500 series XPS with a dual anode x-ray source was used with scans from 0 to 4800 V and a resolution of 0.052 eV. Residual catalyst was determined in the aerosolized MWCNTs as described below for aerosol characterization. Surface area was confirmed by gas adsorption analysis (termed BET analysis) using a MONOSORB Model MS-16 (QuantaChrome Corp., Syosset, NY). Surface characteristics of the MWCNTs were assessed by both SEM and TEM as described below for aerosol characterization.

Aerosol generation and exposure. Inhalation exposure atmospheres were produced by mechanical agitation/resuspension of MWCNTs using a jet mill (Fluid Energy, Hatfield, PA) coupled to a dry chemical screw feeder (Scheck AccuRate, Whitewater, WI) (Cheng *et al*., 1985). Flow through the jet mill was point calibrated to approximately 30 l/min. Aerosols were size classified through a 2-μm cut-point cyclone (Fluid Energy) to ensure that the MWCNTs were in the respirable size range for rodents (approximately < 3 μm). After passing through the cyclone, the aerosols entered an H-2000 2 m^3 whole-body inhalation exposure chamber (Lab Products, Maywood, NJ). The transit time between the jet mill, dilution system, and exposure chamber (~3 s) was minimized to reduce particle agglomeration. Inhalation exposure chambers were maintained at a flow (~0.5 m^3/min) that provided approximately 15 air exchanges per hour. Approximately 100 g MWCNT was consumed during the study.

Atmosphere characterization. Aerosol dilutions were monitored and controlled based on particle mass concentrations measured in both real time and with integrated filter measurements. All aerosol collections were made directly from the breathing zone of the rodents. Particle mass was measured gravimetrically after collection onto Teflon-coated glass fiber filters (Pall-Gelman T60A20, East Hills, NY). Filters were placed in aluminum filter holders and flows were point calibrated to 5 l/min. A nephelometer (DustTrack, TSI Inc., St Paul, MN) was used for real-time measurement of particle mass.

Aerodynamic particle size distribution was determined using a Mercer cascade impactor (In-Tox Products, Moriarty, NM) operated at 2 l/min. Particle number size distribution was determined by a combination of a differential mobility analyzer (3081 DMA, TSI Inc.) and time of flight (3321 APS, TSI Inc.). The combination of the DMA and APS allowed integrated analysis of particle number size distribution from approximately 10 nm to 20 μm.

Particle morphology and structure were analyzed by TEM after collection (10-min collection) by electrostatic precipitation on copper-coated lacey grids (Ted-Pella, Inc., Redding, CA). TEM was conducted using high resolution JEOL 210 at 200 KeV. SEM was conducted using a Hitachi model S-4700 cold field emission SEM with resolutions of 2.5 nm at 1 KeV and 1.5 nm at 15 KeV. SEM images were created using Quartz PCI software (Quartz Imaging Corporation, Vancouver, BC) and TEM images were created using Gatan IV Digital Imaging software (Gatan Inc., Gatan, UK). Qualitative elemental composition of samples on the TEM grid was analyzed by energy-dispersive x-ray spectroscopy (EDS) via an Oxford-LINK Isis instrument. Quantitative analysis of metal impurities was determined by inductively coupled plasma mass spectroscopic (ICPMS) analysis of material collected on Teflon-membrane filters (Pall-Gelman). Approximately 1 mg of material was collected on the Teflon-membrane filters, which were then subjected to acid digestion using a MARSXPress microwave digestion system. The acid digestion cocktail was 14% nitric acid, 6% hydrochloric acid, and 5.0% hydrofluoric acid. Metals were then detected using a PerkinElmer Elan 6000 ICPMS (PerkinElmer, Boston, MA) using commercially available analytical standards (Sigma Aldrich, St Louis, MO).

Estimation of dose. Respiratory minute volume (RMV) was estimated using an allometric equation described by Bide *et al.* (2000). Dose was estimated using the following formula:

$$\text{Dose} = (\text{C} \times \text{RMV} \times \text{T} \times \text{DF})/\text{BW},$$

where C is the average concentration of the MWCNTs in the exposure atmosphere, T is exposure time, and the pulmonary deposition fraction (DF) was assumed to be 10% (Miller, 2000).

Animals. Male C57BL/6 mice ($n = 6$ per group) were obtained from Charles River Laboratories (Portage, MI). Animals were ordered at 8 weeks of age and quarantined for 2 weeks upon arrival. Animal procedures were approved by Lovelace Respiratory Research Institute and University of New Mexico Institutional Animal Care and Use Committees. Animal housing and husbandry was performed in accordance with the *Guide for the Care and Use of Laboratory Animals* (National Research Council, 1996). Mice were exposed 6 h/day for 7 or 14 days and had access to water *ad libitum* during exposures. Standard rodent diet (2016 Global Rodent Diet, Harlan Teklad, Madison, WI) was provided *ad libitum* during nonexposure hours. The morning following the last day of exposure, an overdose of pentobarbital and phenytoin was administered by ip injection. Blood was drawn by cardiac puncture into heparinized syringes. Lungs were removed with the trachea intact. Spleen was collected using aseptic technique.

Lung lavage and pathology. The right cranial lung lobe was ligated and the left lung isolated with a clamp. Remaining right lung lobes were lavaged three times with 0.5 ml of sterile saline. Lavage fluid from the three washes was combined. Viable white blood cells were counted using trypan blue exclusion on a hemocytometer. Cells were spun onto slides using cytofunnels (Shandon, Thermo Corp., Pittsburgh, PA) and differential populations quantified using Diff-Quick stain (Baxter Health, McGaw Park, IL). The right lung was then ligated and removed and the left unclamped and instilled with 10% neutral-buffered formalin (NBF). Right lungs, with the exception of the right cranial lobe, were snap frozen in liquid nitrogen and stored at − 80°C. Right cranial lobes were stored for future use in Karnovsky's fixative. Left lungs were immersed in NBF until sectioning (at least 48 h), and were routinely processed, paraffin embedded, and sectioned at 5 μm. Slides were stained with hematoxylin and eosin and examined by a board certified veterinary pathologist.

Spleen harvest and cell isolation. Spleens were harvested into sterile Hank's Balanced Salt Solution (Cambrex, Walkersville, MD) in a sterile 15-ml centrifuge tube on ice. Using sterile forceps and gauze, spleens were blotted to remove excess liquid and weighed. Once weights were recorded, spleens were bathed in approximately 5 ml of supplemented RPMI media in a sterile culture dish. Supplemented RPMI media contained 10% fetal bovine serum (FBS) (Hyclone, Logan, UT), 1% penicillin/streptomycin (Cambrex), and 1% L-glutamine (Cambrex). Microscope slides were flame sterilized and frosted

ends were used to homogenize the spleen. Isolated splenocytes remained on ice until all samples had been isolated and then were centrifuged at 280 × g for 10 min. Splenocyte pellets were resuspended in 2 ml of supplemented RPMI media. Lymphocytes were counted and viability was determined for each sample by trypan blue exclusion on a hemocytometer. Counts and viabilities were recorded and used for normalizing lymphocyte number during cell plating for immune function assays.

Jerne-Nordin plaque assay. Spleen cells were suspended in 3 ml of supplemented RPMI media at a concentration of 4×10^6 cells/ml. For the Jerne-Nordin plaque assay, supplemented media contained heat inactivated FBS (Hyclone), 1% penicillin/streptomycin (Cambrex), 1% L-glutamine (Cambrex), 0.09% 55mM 2-mercaptoethanol (Gibco, Grand Island, NY), 1% 100mM sodium pyruvate (Cambrex), and 0.5% gentamicin (Gibco).

Sheep red blood cells (SRBC, 1% cells in media) (Colorado Serum, Denver, CO) were washed and suspended in supplemented RPMI media and added to the appropriate wells of a 48-well plate. Each sample was immunized with SRBC in duplicate. SRBC-free media was used for nonimmunized control wells for each sample. Cells were incubated for 4 days in 5% CO_2 at 37°C. Following spleen cell immunization, cells were washed and resuspended in supplemented media. A 0.8% solution of agarose (SeaPlaque, Cambrex, Rockland, ME) in 2 × RPMI medium (Gibco) was warmed to 43°C in glass tubes. SRBC and spleen cells were added to the tubes and then spread on agarose-coated microscope slides and incubated face down on custom slide trays in a humidified plastic box at 37°C for 1 h. Guinea pig complement (Colorado Serum) was diluted 1:20 in Dulbecco's phosphate-buffered saline (PBS) containing Ca^{2+} and Mg^{2+} (Sigma Aldrich) and warmed to 37°C in a water bath. Slides were flooded with diluted complement following the 1-h incubation and then incubated an additional 2 h. Slides were removed from the incubator and stored in a cold 0.85% sodium chloride solution. SRBC lysis was quantified by counting plaques in the SRBC/agar lawn using a dissecting microscope. Control values for the assay are reported and results expressed as percent control.

Mitogenesis assay. For each spleen sample, cells were suspended in 5 ml of supplemented RPMI media at a concentration of 1×10^6 cells/ml. Each spleen sample was tested in replicates of six for three mitogens, for a total of 18 wells per sample. Two hundred microliters (2×10^5 cells) were placed in corresponding wells of sterile flat-bottom 96-well plates. Concanavalin A (Con A) (Sigma Aldrich) was added to wells at a final concentration of 1 μg/ml. Lipopolysaccharide (LPS) (Alexis, San Diego, CA) was added to wells at a final concentration of 10 μg/ml. Supplemented RPMI media were added to control wells. Plates were briefly mixed on a plate shaker and then placed in a 5% CO_2, 37°C incubator for 48 h. Following incubation, the cells were pulsed with 1 μCi per well of ^{3}H-thymidine (MP Biomedicals, Irvine, CA) and incubated for an additional 18 h. Cells were harvested using a Brandel Model 24V cell harvester onto filter paper (Whatman, Maidstone, England) and lysed with a 0.05% Tween 20 solution (Fisher Scientific, Denver, CO). Once samples were completely dry, they were placed in liquid scintillation vials containing 3 ml ScintiVerse Scintillation Cocktail (Fisher Scientific), and counted on a liquid scintillation beta counter. Results for controls are reported and then expressed as percent control based on counts per minute.

Natural killer cell assay. A mouse lymphoma cell line (Yac-1, ATCC, Manassas, VA) was used as a target cell in this assay because it is sensitive to the cytotoxicity of natural killer (NK) cells. Yac-1 cells were incubated with radioactive chromium-51 (PerkinElmer) (50 μCi/1 × 10^5 Yac-1 cells) for 1 h prior to plating. Labeled Yac-1 cells were then plated at a concentration of 5×10^3 cells per well in round-bottom 96-well plates. Splenocytes were plated at 1×10^6 cells/ml for an effector to target ratio (E:T) of 200:1. E:Ts of 200:1, 100:1, 50:1, and 25:1 were plated as an internal control for the assay. In order to measure maximum chromium release, Triton X-100 was added at a concentration of 5% to control wells and spontaneous chromium release was measured by analyzing wells that only contained target and no effector cells. Splenocytes and Yac-1 cells were coincubated for 4 h at which point plates were centrifuged at 200 × g for 10 min. In order to measure chromium release as a result of Yac-1 lysis, supernatants were collected into tubes (PerkinElmer) and analyzed on a gamma counter.

Real-time RT-PCR. Right lung lobes or spleen samples were transferred from − 80°C directly into lysis buffer provided by RNeasy Qiagen Kit (Valencia, CA), and homogenized manually using RNase-free sterile pellet pestles (Kimble/Kontes, Vineland, NJ). RNA was isolated using a standard bench protocol provided with the kit. Total RNA quantity was determined by spectrophotometer (DNanoDrop Technologies, Wilmington, DE). A reverse transcription step was performed on total RNA at a concentration of 8 ng/μl using cDNA archive kit (Applied Biosystems, Foster City, CA). cDNA was amplified 40 times and detected using Universal PCR master mix (Applied Biosystems) and TaqMan primer/probe sets (Applied Biosystems) for indicated genes.

Enzyme-linked immunosorbent assay. Isolated splenocytes were centrifuged and supernatants collected and frozen for protein detection. Ready Set Go ELISA kit for IL-10 (eBioscience, San Diego, CA) was purchased and standard bench protocol provided by the kit was used. Briefly, 96-well plates were coated overnight at 4°C with mouse IL-10 capture antibody. Plates were washed five times with a wash buffer containing 0.05% Tween 20 (Fisher Scientific) in Dulbecco's PBS (Sigma Aldrich). Plates were then blocked for 1 h with assay diluent provided with the kit and washed five times. One hundred microliters of sample or IL-10 standard provided by the kit was added per well and incubated overnight at 4°C followed by five washes. Plates were incubated for 1 h with 100 μl per well biotin-labeled detection antibody and washed five times. Plates were incubated with 100 μl per well avidin/HRP for 30 min then washed 14 times. One hundred microliters per well of substrate solution was added and incubated for 15 min followed by addition of 50 μl stop solution, 2M sulfuric acid. Plates were read on a 96-well plate reader at 450 nm with 570-nm wavelength subtraction. Sample readings were quantified using a standard curve and expressed as percent control.

Statistical analysis. All assays were run with $n = 6$ per group with the exception of the ELISA, where an $n = 3$ was used due to limited sample. Differences among treatment groups were tested by one-way ANOVA using SigmaStat software version 3.5 (Systat Software Inc., Richmond, CA). Error bars indicate the SE of the samples. Criterion for biostatistical significance was set at $p = 0.05$.

RESULTS

MWCNT Bulk Characterization

Table 1 summarizes the manufacturer's specifications of the MWCNTs and the additional analytical results we obtained. BET surface area of the MWCNTs was determined to be 100 m^2/g (manufacturer's specifications ranged from 40 to 300 m^2/g). TEM and SEM analysis of the bulk material (Fig. 2) showed a high purity for the MWCNTs with little indication of impurities due to metal catalyst, oxide, or ash. The SEM revealed the clumping of bulk material. TEM showed a range of diameters (~10–20 nm; ~20 nm shown), with each tube structure defined by herringbone-shaped carbon layers. The herringbone structure is one of many carbon layer structures previously observed in MWCNTs and other carbon nanofibers (Vander Wal *et al*., 2002). The length of the individual tubes were not measured (manufacturer specifications indicate they are ~5–15 μm in length). It was also noted that nanotubes did not appear to be rigid, but instead they were flexible and the majority were coiled into agglomerates that were less than

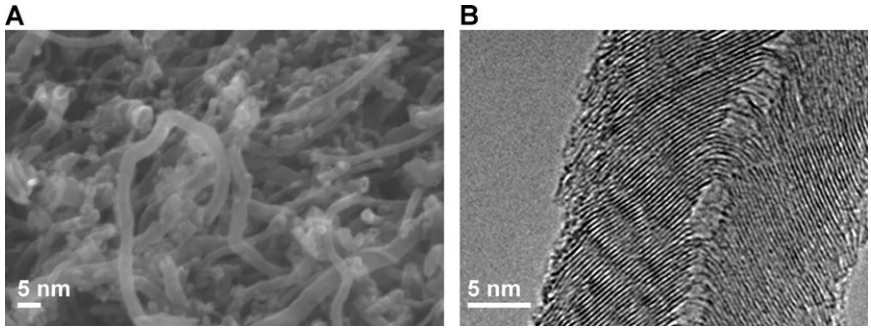

FIG. 2. Images of MWCNT bulk material by (A) SEM and (B) TEM. MWCNT are provided from the vendor as agglomerated powders. As shown in (A), the MWCNT are not completely rigid and bend together into a mesh. Panel B illustrates the diameter and structure of individual MWCNT, showing an approximately 20-nm–wide MWCNT possessing a herringbone-shaped carbon lamella.

1 μm. XPS analysis revealed high carbon purity (> 97%), with little indication of impurities (Table 1). As indicated below for aerosol characterization, more sensitive methods did detect small quantities of metal impurities.

Aerosol Concentration and Characteristics

Average MWCNT particle concentrations for the 14-day inhalation exposure were (mean ± SD) 0 (control), 0.3 ± 0.1, 1.0 ± 0.1, and 5.3 ± 0.6 mg/m^3. Electron microscopy (Fig. 3) showed that the MWCNT aerosols were a mixture of material in varying states of agglomeration (clumping), including some tubes that were not agglomerated. The agglomeration increased with increasing aerosol concentration. The mass median aerodynamic particle diameter was approximately 0.7–1 μm (~2.0 geometric SD) for the 0.3- and 1-mg/m^3 exposure and 1.8 μm (2.5 geometric SD) for the 5-mg/m^3 exposure. Particle number size distribution was smaller, with a median at approximately 350–400 nm at the 1-mg/m^3 exposure level (Fig. 4).

EDS analysis of MWCNTs on TEM grids (Fig. 5) revealed the presence of nickel and iron impurities. These metals were used as catalysts by the manufacturer during the CVD synthesis of the MWCNTs. ICPMS analysis showed that nickel and iron each accounted for approximately 0.5 % of the particle mass in the aerosol. No other metals were observed at concentrations above the detection limits of the ICPMS.

Bronchial Alveolar Lavage Fluid

Analysis of BALF showed clear evidence of MWCNTs engulfed by macrophages (Fig. 6). At the 5-mg/m^3 exposure level, macrophages appeared to be heavily loaded with particles. However, there was no increase in inflammatory cells in the lung as a result of MWCNT exposure, and no change in the distribution of cell types relative to nonexposed animals (Table 2).

Pulmonary Histopathology

Figure 7 compares control versus the 5-mg/m^3 exposure group at increasing magnifications (images taken using 4, 10, and 40 × objectives). Control and exposed lung sections looked very similar at low magnifications (panels A, B, D, and E; 4 and 10 × objective), illustrating the lack of severe inflammation and tissue injury and an absence of large aggregates of particles. The inhalation exposure provided good distribution of MWCNTs throughout the lung. At higher magnification (40 × objective, panels C and F) the MWCNTs can be observed. These MWCNTs were found primarily as aggregates

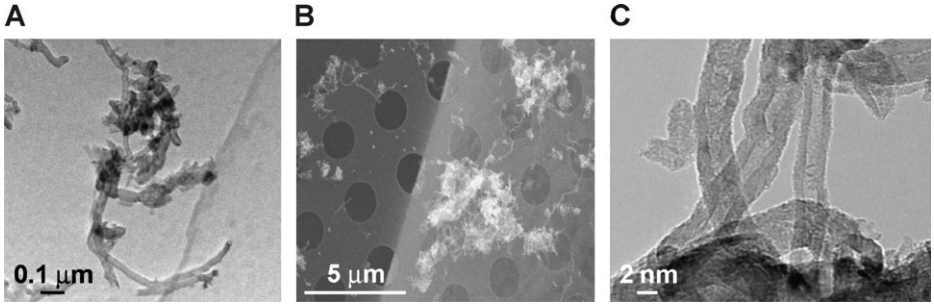

FIG. 3. Electron micrographs of MWCNTs collected after aerosolization from inhalation exposure atmospheres, size selected by passing through a 2-μm cut-point cyclone, and diluted to 1 mg/m^3 (A–C). Reference bars are shown for each image. The majority of the MWCNT were agglomerated into clumps. As shown, the material were not rigid, they were rather flexible. While material agglomerates, the aerosolization procedure did not appear to damage or fracture any of the MWCNT (compared with Fig. 2).

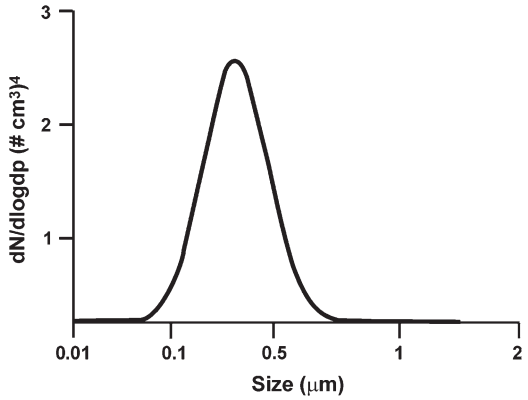

FIG. 4. Particle number size distribution analyzed by differential mobility and time of flight for MWCNTs aerosolized, transported through a 2-μm size selective cyclone, and diluted to 1 mg/m^3.

that were in macrophages. A few free MWCNTs were also observed. The amount of material apparent on light microscopic exam was qualitatively correlated with exposure concentrations. Although, as expected, with increased exposure an increased number of particles were observed in the lung. Because no indications of fibrosis, increased cellularity, or granuloma formation were observed by light microscopic analysis at the highest exposure group, only sections from that group are shown. As indicated, most of the visible material was present within alveolar macrophages, with lesser amounts noted extracellularly on surfaces, and none noted within other cell types. There were only minor amounts of the MWCNTs observed in the conducting airways, and there was a minimal tendency for macrophages to accumulate in the region of the alveolar ducts. While macrophages containing MWCNTs were more visible in histologic sections, a substantiative increase in macrophage numbers was not observed (similar to the observation in BALF).

Systemic Immune Function

Mice exposed to MWCNTs for 7 days did not have altered immune function in any of the treatment groups (data not shown). Mice exposed for 14 consecutive days, at all MWCNT concentrations, demonstrated a suppressed T-cell–dependent antigen response (Fig. 8A). Plaque-forming cell cultures for an average control-treated animal were in the range of 500–600 plaques per culture, a common range for this assay. Results are expressed as percent control. Figure 8B shows that exposed T cells had reduced proliferative ability, as illustrated by the reduction in response to mitogen (Con A). Results were collected as counts per minute (average LPS response was 20,000 cpm for control animals) and expressed as percent control. B-cell proliferation (LPS stimulation) was unaffected (Fig. 8B). NK cell–mediated lysis of Yac-1 target cells, a measure of innate immune response, was suppressed by MWCNT inhalation only at the 1-mg/m^3 concentration (Fig. 8C).

Gene and Protein Expression

IL-6, IL-10, and NAD(P)H oxidoreductase 1 (NQO1) mRNA expression was not increased in the lung following inhalation of MWCNTs for 7 or 14 days (data not shown). However, spleen mRNA levels for IL-10 and NQO1 were increased significantly ($p < 0.05$) with 14-day MWCNT exposure (Fig. 9A). The mRNA results observed for IL-10 were confirmed with IL-10 protein analysis by ELISA, which showed an increase in IL-10 protein at 1 and 5 mg/m^3 (Fig. 9B).

DISCUSSION

Inhalation of MWCNTs for 14 days up to the current occupational exposure guideline for human exposure to nuisance

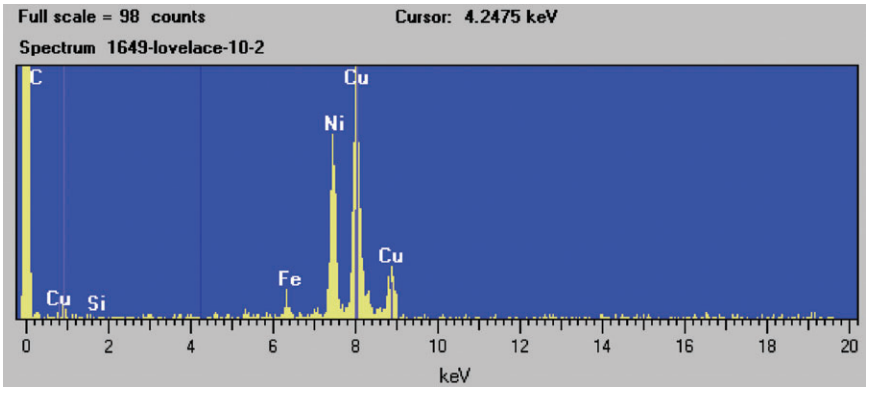

FIG. 5. EDS of TEM sample of MWCNTS from the 1-mg/m^3 exposure atmosphere. Copper peak is due to the background from the collection grid. Spectral analysis shows presence of nickel and trace amounts of iron, both catalysts used in the synthesis of MWCNTs. Large carbon peak (left) is from the carbon structure of MWCNTs.

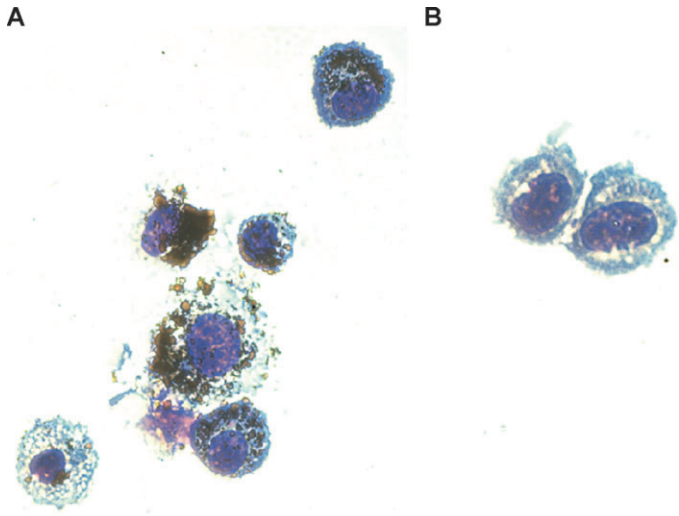

FIG. 6. Representative images from BALF collected from animals exposed for 14 days to 5-mg/m^3 (A) MWCNT and (B) controls. BALF from exposed lungs contained many particle-laden and some enlarged macrophages.

dusts (5 mg/m^3) (NIOSH, 2005) did not result in lung damage using the measurements described above but did affect systemic immunity. Immune function measurements on spleen-derived cells showed suppressed T-cell–dependent antibody response, decreased proliferation of T cells following mitogen stimulation, and altered NK cell killing. These results were accompanied by increased NQO1 and IL-10 gene expression (indicators of oxidative stress and altered immune function, respectively) in the spleen, but not in the lung.

The absence of pulmonary effects, even at relatively high exposure concentrations, contrasts with many of the findings associated with the pulmonary toxicity of CNTs reported to date. Others have reported significant inflammation, oxidative stress, and tissue injury resulting from CNT instillations and pharyngeal aspirations. These previous studies included rats and mice receiving instilled or aspirated doses of 1–5 mg/kg of SWCNTs (Lam *et al*., 2004; Shvedova *et al*., 2005; Warheit *et al*., 2004) and rats instilled with MWCNTs up to approximately 10 mg/kg (Muller *et al*., 2005). All these previous studies reported significant granuloma formation, and some studies observed fibrosis in combination with the granulomas (Shvedova *et al*., 2005). There was significant variation in the response to CNTs obtained from different sources, which Lam *et al*. (2004) attributed to residual metal content for the SWCNTs. Muller *et al*. (2005) reported the only MWCNT results and showed an increase in lung pathology and inflammation at approximately 10 mg/kg, but not in the 2-mg/kg range. MWCNT toxicity was increased when physically ground into smaller agglomerates (Muller *et al*., 2005). In most cases, both SWCNTs and MWCNTs at high bolus doses resulted in significant lung pathology within a short time period (days to weeks). When the rodents were monitored for several months, the tissue injury progressed.

TABLE 2
BALF Cell Differentials Collected from Three Washes of Right Lung Lobes Did Not Show a Change in the Composition of Lavage Cells with MWCNT Exposure

	Percent			
Exposure	Macrophages	PMNs	Lymphocytes	Eosinophils
Control	100 ± 0	0	0	0
0.3 mg/m^3	99.17 ± 1.33	0.67 ± 1.2	0.17 ± .41	0
1 mg/m^3	100 ± 0	0	0	0
5 mg/m^3	97.17 ± 2.04	0.99 ± 1.26	1.84 ± 1.48	0

Note. Results are expressed as average cell percentage observed in BALF ($n = 6$) ± SD.

The absence of inflammation and significant pathology for the MWCNT inhalation study described herein is not surprising. As for silica and some other materials, the response to inhaled CNTs may manifest over several months (Langley *et al*., 2004) and was only analyzed at 14 days. Based on the dramatic (and early) responses by instillation or aspiration reported in the literature, it was originally thought that we would observe some pathology and inflammation even at early time points. The estimated deposited doses for this study were 0.2, 0.5, and 2.7 mg/kg at the 0.3-, 1-, and 5-mg/m^3 exposure levels, respectively. While the highest exposure concentration mimics the current occupational exposure guideline for nuisance dusts (applied to CNTs in the absence of a specific standard), it is approximately 100 times the concentration of CNTs found in an industrial hygiene report by Maynard *et al*. (2004). The justification for higher exposure concentrations may be difficult, especially considering the potential for false positives that may result from overload of particles in the lung (Mossman, 2000; Oberdorster, 2002). The dramatic effects that have been reported in the literature for MWCNTs have been typically only reported at doses well above our highest estimated dose.

In addition to differences in response between this study and previous reports that may be attributed to dose, specific type, and functionalization of CNTs, an important consideration is the route of administration. While instillation has commonly been used to compare particles of different types (Henderson, 1995; Seagrave *et al*., 2002), the use of instilled or aspirated CNTs may be complicated by their poor solubility, which makes creation of homogenous and well-dispersed dosing suspensions difficult. Instillation, and to a lesser extent aspiration, results in the agglomeration of material (albeit particle size in solution not reported in aforementioned publications on CNT instillations and aspirations). This suspension is placed either directly into the lung or on the back of the tongue and may lead to granuloma formation because large concentrations of material collect in specific foci which result in a "foreign body" type response.

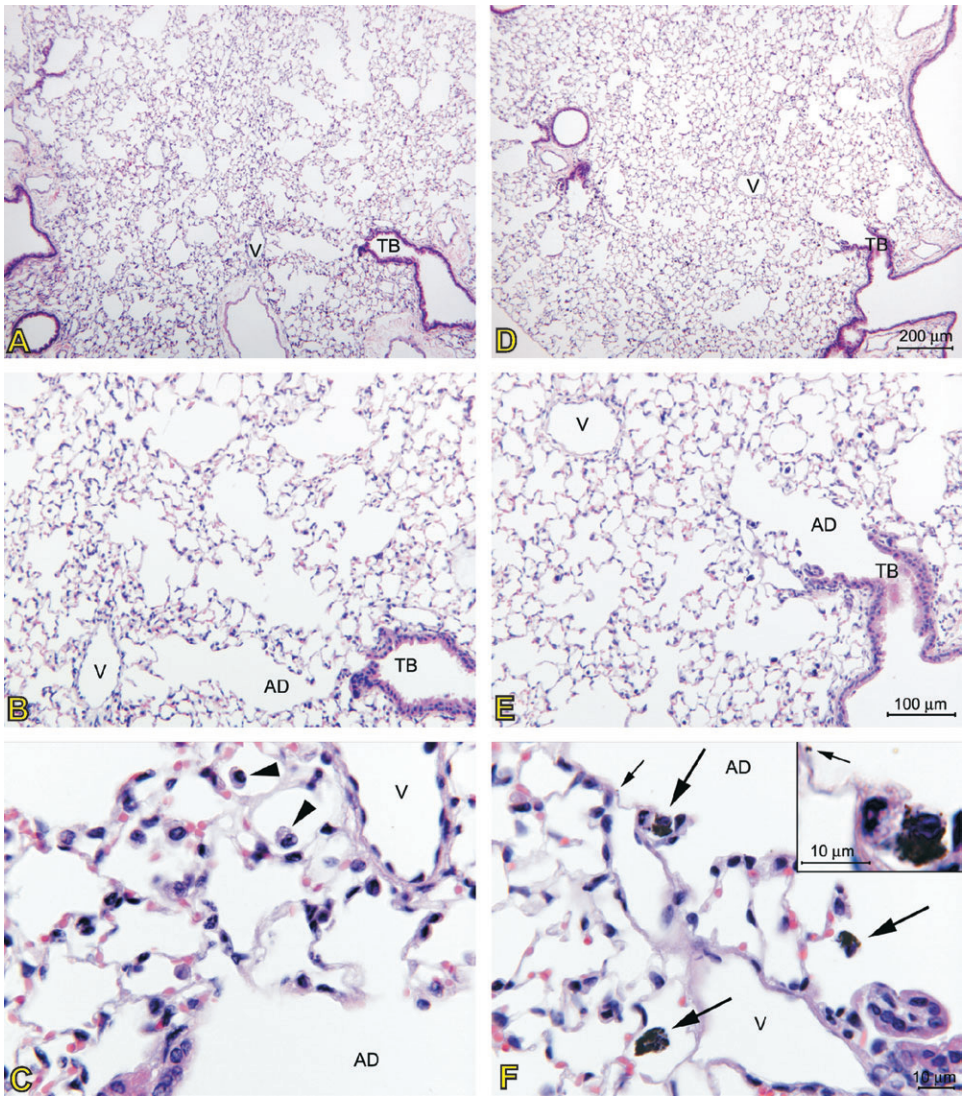

FIG. 7. Representative hematoxylin and eosin–stained lung sections at equivalent magnifications from a control animal (panels A, B, and C) and an animal exposed to 5 mg/m^3 MWCNTs for 14 consecutive days (panels D, E, and F) by inhalation. Note the unremarkable appearance of the lung from the exposed animal at low magnification (panels D and E), including the alveolar duct regions. At increasing magnification, alveolar macrophages from control lungs are unremarkable (arrowheads), while dark, particulate-laden macrophages become evident in exposed animals (large arrows). Scattered particulate material is also present on surfaces (small arrows). However, no substantive lung damage or cellularity increase is apparent with exposure in this study. (V, vessel; TB, terminal bronchial; AD, alveolar duct. Magnifications as indicated by bars).

A relevant example is that of diesel particles, a carbonaceous material that is different from CNTs but has similar properties in solution (forms agglomerates due to poor solubility and Van der Waal's forces). Diesel particles will cause granulomas (similar to what have been reported for CNTs) when administered by instillation (Seagrave *et al*., 2002). In contrast, inhalation of diesel exhaust (DE) at occupational exposure levels did not lead to persistent lung inflammation, tissue injury, or granuloma formation (Reed *et al*., 2004). Furthermore, Reed *et al*. (2004) did show macrophages laden with diesel particles, but did not find an increase in macrophage number in the lung after inhalation exposure durations for 1 week or 6 months. During histopathological analysis, we observed most of the MWCNTs in the alveolar region and not in the conducting airways. Deposition in conducting airways is often observed when particles are administered by instillation. It is plausible that even with CNTs that may be more toxic than the MWCNTs we studied here, tissue injury would be dramatically reduced if administered by inhalation.

We have previously reported impaired immune function following inhalation of carbonaceous particles in environmentally relevant materials such as DE and wood smoke. After 6-month exposures to hardwood smoke, AJ mice had suppressed T-cell mitogenic response. This was determined to be

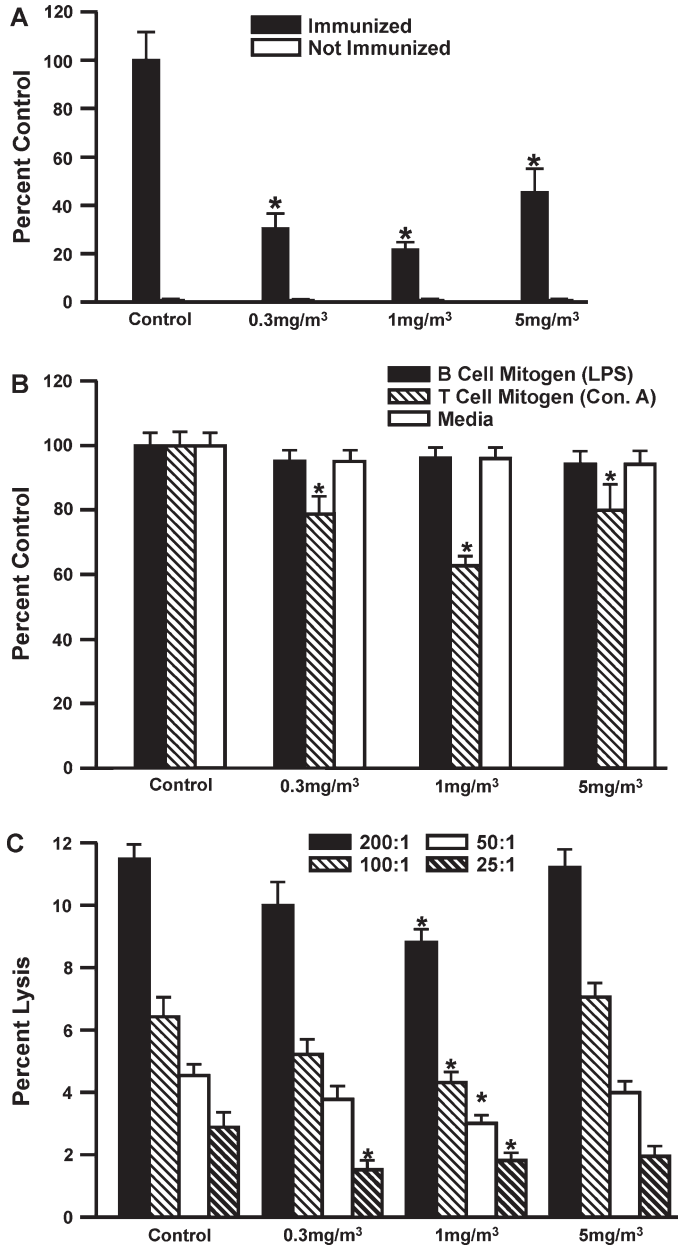

FIG. 8. (A) Jerne-Nordin plaque assay results following 4-day immunization with sheep erythrocytes (SRBC). Plaque number per culture was decreased with exposure (25–45% of control). Each sample was assayed without SRBC immunization as a negative control. (B) T- and B-cell proliferation in response to cell-specific mitogen was analyzed using tritiated thymidine incorporation. T-cell proliferation in response to Con A was decreased with MWCNT exposure. (C) NK cell function, as measured by target cell lysis, was suppressed with exposure. Effector: Target ratios ranging from 200:1 down to 25:1 serve as a quality control measure for the assay. *Signifies statistically significant difference ($p < 0.05$), $n = 6$.

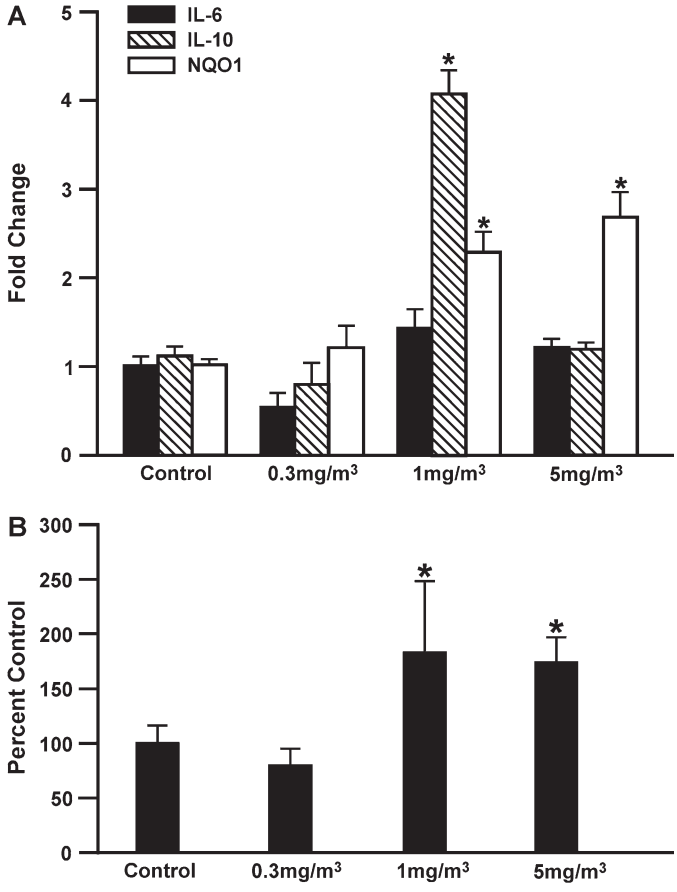

FIG. 9. (A) Interleukin cytokines IL-6 and IL-10 and electrophile response gene NQO1 were measured in spleen homogenate. Splenic mRNA expression for IL-10 and NQO1 was increased with exposure ($n = 6$). (B) IL-10 protein, as measured by ELISA with splenocyte supernatant, was increased with exposure to MWCNTs. *Signifies statistically significant difference ($p < 0.05$), $n = 3$.

from altered immune cell function and not due to lymphocyte cell death (Burchiel *et al.*, 2004). Six-month exposures to DE resulted in suppressed splenic T-cell mitogenic responses as well (Burchiel *et al.*, 2005). In those studies it was not determined if the particles or gaseous components of the exposures caused the immune suppression. If the particles did play a role, then it may be plausible that the mechanism of MWCNT-induced immune suppression is similar. However, this has not been tested.

Others have shown increased oxidative stress and increased IL-10 levels with carbon-based particle exposures (Harris *et al.*, 1997a,b; Li *et al.*, 2002, 2003; Pacheco *et al.*, 2001; Ullrich and Lyons, 2000). Following particle exposures *in vivo*, Harris *et al.* (1997a,b) noted immunosuppression in animals following inhalation exposures to high doses of aerosolized jet propulsion fuel (JP-8) that was linked to T-cell dysfunction. This observation was later expanded by Ullrich and Lyons (2000) and linked to IL-10 production. IL-10 is an anti-inflammatory cytokine principally secreted by macrophages and T cells (T-helper type 2 [TH2]). Its activity serves to downregulate cytokines such as IL-12, TNF-α, IFN-γ, and IL-1β (Yin *et al.*, 1997a,b). Although the role of IL-10 in modulating the immune response to MWCNTs has not been confirmed, its upregulation

in the spleen was intriguing. Furthermore, IL-10 and NQO1 expression in the spleen, not observed in the lung, suggests that MWCNTs are potentially bypassing pulmonary defense mechanisms and reaching circulation. This is further evidenced by a lack of cellular influx and IL-6 expression in the lung. Within the systemic framework, MWCNTs may induce oxidative stress and/or activate electrophile response pathways resulting in NQO1 and simultaneous or consequent IL-10 expression.

IL-10 is a very important regulator of the immune system and serves to maintain homeostatic control of innate and cell-mediated immune responses. However, if IL-10 is inappropriately expressed, as shown in this study, it may suppress normal immune response and increase susceptibility to infection and disease. The complexity of the immune system is such that suppression on the level of innate immunity results in affects on a humoral level as well. The Jerne-Nordin plaque assay is an evidence for immune cell interaction, where T-helper cell activation in presence of antigen, SRBC, results in communication with B cells to induce IgM antibody production. However, IgM induction is a T-helper cell type 1 (TH1) effect; IL-10 is involved in TH2 polarization and therefore results in suppression of the IgM response as well as decreased antiviral, antitumor, and intracellular microbe killing. IL-10 expression has been linked to diabetes promotion (Balasa *et al*., 2000) and cancer risk (Mustea *et al*., 2006) in humans. IL-10 has also been shown to increase atopy by enhancement of IgE secretion by B lymphocytes (Ohmori *et al*., 1995; Prasse *et al*., 2007).

Several questions arise from the observations of immune suppression related to exposure to CNTs and environmental pollutants. First, the immune function responses observed in the spleen have not been evaluated in other parts of the body, such as in the lymph nodes or in immune cells in the lung. Many questions exist regarding the mechanism by which this immune suppression occurs. Certainly, there is evidence that exposure to inhaled materials may perturb the ability to fight infection, as evidenced by both animal and epidemiological air pollution studies (Harrod *et al*., 2003, 2005; Shay *et al*., 1999). While the reports by Shvedova *et al*. (2005) suggest a decreased ability to clear *Listeria* bacteria from the lung after SWCNT exposure, that study design may have focused more on evaluating a decreased macrophage function (ability to clear bacteria), possibly due to particle overload, than on a suppressed immune system.

A key component of our study was development of an aerosol generation and inhalation exposure system suitable for CNT rodent exposures. The exposure system was designed to simulate a potential exposure to MWCNTs in the workplace or by an end user prior to functionalization and integration into a product. As such, the approach used powder resuspension of bulk material using a well-tested aerosol generator (Cheng *et al*., 1985). The system was operated with an ~2-μm cut-point cyclone in line to remove particles that agglomerated and those larger than the size a rodent can inhale. While the energy and dilution was designed to minimize excessive agglomeration of the MWCNTs, there were no attempts to intentionally aerosolize ''singlet,'' nonagglomerated MWCNTs. The aerosol that was produced showed reasonable agreement with the limited amount of industrial hygiene measurements of CNTs that have been produced (Maynard *et al*., 2004). Maynard *et al*. (2004) reported a submicron size distribution (based on number) that changed dependent on the amount of artificial agitation applied. Our system also showed a submicron aerosol (based on number), with particles residing primarily at about 300–400 nm. When sized by mass, they were approximately 1–2 μm in diameter. The aerosol consisted of a mixture of a small number of individual tubes and a large amount (by mass) of tubes that agglomerated. This property was desirable, as particles will also most likely exist in an agglomerated state when humans are exposed to them. The agglomeration, as indicated by particle size, increased at the highest exposure concentration.

Characterization showed approximately 99% pure CNTs, with only 1% residual metals (nickel and iron) that are used as catalysts during CVD synthesis. Overall, the system was judged suitable for application of hazard assessment for a wide range of CNTs to represent potential occupational exposures.

This study served to improve the overall understanding of the hazard associated with inhalation of CNTs. While the results of the MWCNTs used in this study may not represent the biocompatibility of other CNTs, this work provides a start toward placing some of the findings presented by instillation in context of exposure to a well-dispersed aerosol. More work needs to be done to evaluate the role of CNTs of various compositions and all CNTs using study designs that evaluate the potential for progressive injury. Certainly, the findings of immune suppression, cytokine upregulation, and oxidative stress in the spleen were intriguing. The immune suppression was observed even at the lower exposure levels. Further work is necessary to place these results in context, and to further elucidate a mechanism for this response.

FUNDING

Environmental Protection Agency (RD-83252701-0); National Institute for Environmental Health Sciences (P30-ES012072, 5 S11 ES013339-03).

REFERENCES

Balasa, B., La Cava, A., Van Gunst, K., Mocnik, L., Balakrishna, D., Nguyen, N., Tucker, L., and Sarvetnick, N. (2000). A mechanism for IL-10-mediated diabetes in the nonobese diabetic (NOD) mouse: ICAM-1 deficiency blocks accelerated diabetes. *J. Immunol.* **165,** 7330–7337.

Bide, R. W., Armour, S. J., and Yee, E. (2000). Allometric respiration/body mass data for animals to be used for estimates of inhalation toxicity to young adult humans. *J. Appl. Toxicol.* **20,** 273–290.

Burchiel, S. W., Lauer, F. T., Dunaway, S. L., Zawadzki, J., McDonald, J. D., and Reed, M. D. (2005). Hardwood smoke alters murine splenic T cell responses to mitogens following a 6-month whole body inhalation exposure. *Toxicol. Appl. Pharmacol.* **202,** 229–236.

Burchiel, S. W., Lauer, F. T., McDonald, J. D., and Reed, M. D. (2004). Systemic immunotoxicity in AJ mice following 6-month whole body inhalation exposure to diesel exhaust. *Toxicol. Appl. Pharmacol.* **196,** 337–345.

Cheng, Y. S., Marshall, T. C., Henderson, R. F., and Newton, G. J. (1985). Use of a jet mill for dispersing dry powder for inhalation studies. *Am. Ind. Hyg. Assoc. J.* **46,** 449–454.

Harper, T. E., and Vas, C. R. (2005). From polymer chemistry to nanotechnology: The return of the renaissance scientist? *Abstr. Pap. Am. Chem. Soc.* **229,** U906.

Harris, D. T., Sakiestewa, D., Robledo, R. F., and Witten, M. (1997a). Immunotoxicological effects of JP-8 jet fuel exposure. *Toxicol. Ind. Health* **13,** 43–55.

Harris, D. T., Sakiestewa, D., Robledo, R. F., and Witten, M. (1997b). Short-term exposure to JP-8 jet fuel results in long-term immunotoxicity. *Toxicol. Ind. Health* **13,** 559–570.

Harrod, K. S., Jaramillo, R. J., Berger, J. A., Gigliotti, A. P., Seilkop, S. K., and Reed, M. D. (2005). Inhaled diesel engine emissions reduce bacterial clearance and exacerbate lung disease to Pseudomonas aeruginosa infection in vivo. *Toxicol. Sci.* **83,** 155–165.

Harrod, K. S., Jaramillo, R. J., Rosenberger, C. L., Wang, S. Z., Berger, J. A., McDonald, J. D., and Reed, M. D. (2003). Increased susceptibility to RSV infection by exposure to inhaled diesel engine emissions. *Am. J. Respir. Cell Mol. Biol.* **28,** 451–463.

Henderson, L. W. (1995). Why do we use 'clearance'? *Blood Purif.* **13,** 283–288.

Huczko, A., Lange, H., Calko, E., Grubek-Jaworska, H., and Droszcz, P. (2001). Physiological testing of carbon nanotubes: Are they asbestos-like? *Fullerene Sci. Tech.* **2,** 251–254.

Kipen, H. M., and Laskin, D. L. (2005). Smaller is not always better: Nanotechnology yields nanotoxicology. *Am. J. Physiol. Lung Cell. Mol. Physiol.* **289,** L696–L697.

Lam, C. W., James, J. T., McCluskey, R., Arepalli, S., and Hunter, R. L. (2006). A review of carbon nanotube toxicity and assessment of potential occupational and environmental health risks. *Crit. Rev. Toxicol.* **36,** 189–217.

Lam, C. W., James, J. T., McCluskey, R., and Hunter, R. L. (2004). Pulmonary toxicity of single-wall carbon nanotubes in mice 7 and 90 days after intratracheal instillation. *Toxicol. Sci.* **77,** 126–134.

Langley, R. J., Kalra, R., Mishra, N. C., Hahn, F. F., Razani-Boroujerdi, S., Singh, S. P., Benson, J. M., Pena-Philippides, J. C., Barr, E. B., and Sopori, M. L. (2004). A biphasic response to silica: I. Immunostimulation is restricted to the early stage of silicosis in Lewis rats. *Am. J. Respir. Cell Mol. Biol.* **30,** 823–829.

Li, N., Kim, S., Wang, M., Froines, J., Sioutas, C., and Nel, A. (2002). Use of a stratified oxidative stress model to study the biological effects of ambient concentrated and diesel exhaust particulate matter. *Inhal. Toxicol.* **14,** 459–486.

Li, N., Sioutas, C., Cho, A., Schmitz, D., Misra, C., Sempf, J., Wang, M., Oberley, T., Froines, J., and Nel, A. (2003). Ultrafine particulate pollutants induce oxidative stress and mitochondrial damage. *Environ. Health Perspect.* **111,** 455–460.

Magrez, A., Kasas, S., Salicio, V., Pasquier, N., Seo, J. W., Celio, M., Catsicas, S., Schwaller, B., and Forro, L. (2006). Cellular toxicity of carbon-based nanomaterials. *Nano Lett.* **6,** 1121–1125.

Maynard, A. D., Baron, P. A., Foley, M., Shvedova, A. A., Kisin, E. R., and Castranova, V. (2004). Exposure to carbon nanotube material: Aerosol release during the handling of unrefined single-walled carbon nanotube material. *J. Toxicol. Environ. Health A* **67,** 87–107.

McClellan, R. O. (1994). Assessing health risks of synthetic vitreous fibers: An integrative approach. *Regul. Toxicol. Pharmacol.* **20,** S121–S134.

Miller, F. J. (2000). Dosimetry of particles in laboratory animals and humans in relationship to issues surrounding lung overload and human health risk assessment: A critical review. *Inhal. Toxicol.* **12,** 19–57.

Mossman, B. T. (2000). Mechanisms of action of poorly soluble particulates in overload-related lung pathology. *Inhal. Toxicol.* **12,** 141–148.

Muller, J., Huaux, F., Moreau, N., Misson, P., Heilier, J. F., Delos, M., Arras, M., Fonseca, A., Nagy, J. B., and Lison, D. (2005). Respiratory toxicity of multi-wall carbon nanotubes. *Toxicol. Appl. Pharmacol.* **207,** 221–231.

Murr, L. E., Garza, K. M., Soto, K. F., Carrasco, A., Powell, T. G., Ramirez, D. A., Guerrero, P. A., Lopez, D. A., and Venzor, J. (2005). Cytotoxicity assessment of some carbon nanotubes and related carbon nanoparticle aggregates and the implications for anthropogenic carbon nanotube aggregates in the environment. *Int. J. Environ. Res. Public Health* **2,** 31–42.

Mustea, A., Konsgen, D., Braicu, E. I., Pirvulescu, C., Sun, P., Sofroni, D., Lichtenegger, W., and Sehouli, J. (2006). Expression of IL-10 in patients with ovarian carcinoma. *Anticancer Res.* **26,** 1715–1718.

National Institute for Occupational Safety and Health (NIOSH). (2005). *NIOSH Pocket Guide to Chemical Hazards* DDHS No. 2005-149.

National Research Council. (1996). *Guide for the Care and Use of Laboratory Animals*. National Academy Press, Washington, DC.

Oberdorster, G. (2002). Toxicokinetics and effects of fibrous and nonfibrous particles. *Inhal. Toxicol.* **14,** 29–56.

Ohmori, H., Kanda, T., Takai, T., and Hikida, M. (1995). Induction of antigen-specific IgE response in murine lymphocytes by IL-10. *Immunol. Lett.* **47,** 127–132.

Pacheco, K. A., Tarkowski, M., Sterritt, C., Negri, J., Rosenwasser, L. J., and Borish, L. (2001). The influence of diesel exhaust particles on mononuclear phagocytic cell-derived cytokines: IL-10, TGF-beta and IL-1 beta. *Clin. Exp. Immunol.* **126,** 374–383.

Prasse, A., Germann, M., Pechkovsky, D. V., Markert, A., Verres, T., Stahl, M., Melchers, I., Luttmann, W., Muller-Quernheim, J., and Zissel, G. (2007). IL-10-producing monocytes differentiate to alternatively activated macrophages and are increased in atopic patients. *J. Allergy Clin. Immunol.* **119,** 464–471.

Reed, M. D., Gigliotti, A. P., McDonald, J. D., Seagrave, J. C., Seilkop, S. K., and Mauderly, J. L. (2004). Health effects of subchronic exposure to environmental levels of diesel exhaust. *Inhal. Toxicol.* **16,** 177–193.

Rosenthal, G. J., Corsini, E., and Simeonova, P. (1998). Selected new developments in asbestos immunotoxicity. *Environ. Health Perspect.* **106**(Suppl. 1), 159–169.

Seagrave, J., McDonald, J. D., Gigliotti, A. P., Nikula, K. J., Seilkop, S. K., Gurevich, M., and Mauderly, J. L. (2002). Mutagenicity and in vivo toxicity of combined particulate and semivolatile organic fractions of gasoline and diesel engine emissions. *Toxicol. Sci.* **70,** 212–226.

Shay, D. K., Holman, R. C., Newman, R. D., Liu, L. L., Stout, J. W., and Anderson, L. J. (1999). Bronchiolitis-associated hospitalizations among US children, 1980–1996. *JAMA* **282,** 1440–1446.

Shvedova, A. A., Kisin, E. R., Mercer, R., Murray, A. R., Johnson, V. J., Potapovich, A. I., Tyurina, Y. Y., Gorelik, O., Arepalli, S., Schwegler-Berry, D., *et al.* (2005). Unusual inflammatory and fibrogenic pulmonary responses to single-walled carbon nanotubes in mice. *Am. J. Physiol. Lung Cell. Mol. Physiol.* **289,** L698–L708.

Ullrich, S. E., and Lyons, H. J. (2000). Mechanisms involved in the immunotoxicity induced by dermal application of JP-8 jet fuel. *Toxicol. Sci.* **58,** 290–298.

Vander Wal, R. L., Hall, L. J., and Berger, G. M. (2002). Optimization of flame synthesis for carbon nanotubes using supported catalysts. *J. Phys. Chem.* **106,** 13122–13132.

Warheit, D. B., Laurence, B. R., Reed, K. L., Roach, D. H., Reynolds, G. A., and Webb, T. R. (2004). Comparative pulmonary toxicity assessment of single-wall carbon nanotubes in rats. *Toxicol. Sci.* **77,** 117–125.

Yin, Z., Braun, J., Neure, L., Wu, P., Eggens, U., Krause, A., Kamradt, T., and Sieper, J. (1997). T cell cytokine pattern in the joints of patients with Lyme arthritis and its regulation by cytokines and anticytokines. *Arthritis Rheum.* **40,** 69–79.

Yin, Z., Braun, J., Neure, L., Wu, P., Liu, L., Eggens, U., and Sieper, J. (1997). Crucial role of interleukin-10/interleukin-12 balance in the regulation of the type 2 T helper cytokine response in reactive arthritis. *Arthritis Rheum.* **40,** 1788–1797.